



Processing, rheology and structure of melt compounded PBT-clay nanocomposites having different chemical composition.

Luigi Scatteia,¹ Paola Scarfato,^{2*} Domenico Acierno³

¹CIRA – Italian Aerospace Research Centre, Via Maiorise, 81043 Capua (CE), Italy; Fax: (+39) 0823 623515; e-mail: l.scatteia@cira.it

^{2*}Department of Chemical and Food Engineering, University of Salerno, Via Ponte don Melillo, 84084 Fisciano (SA), Italy; Fax: (+39) 089 964057; e-mail: pscarfato@unisa.it

³Department of Materials and Production Engineering, University of Naples “Federico II”, P.le Tecchio 80, 80125 Napoli, Italy; Fax: (+39) 081 7682404; e-mail: acierno@unina.it

(Received: 27 January, 2006; published: 29 May, 2006)

Abstract: In this study the melt flow behavior of poly(butylene terephthalate)–clay nanocomposites produced by melt compounding was investigated. Four commercial organo-modified montmorillonites, differing mainly by the organic treatment used in the modification, were employed as nanometric fillers and blended with the poly(butylene terephthalate) (PBT) at two weight percentages each (6 and 9wt%). The process was carried out using a laboratory-scale twin-screw extruder at two different extrusion rates, in order to evaluate the effect of the shear rate during the process on microstructure and flow properties. In this regard, the nanocomposite samples were submitted to morphological analyses and rheological measurements in the dynamic regime. The effect of temperature on the flow behavior of the hybrids with respect to the neat PBT matrix was also investigated. The obtained data were related to the hybrid compositions and then to the chemical affinity between polymer and clay type. All the reported results have shown a gradual transition from a pseudo-Newtonian trend towards a pseudo-solid-like flow behavior with the increase of the clay loading and the dispersion/exfoliation level of the clay particles, due to the corresponding increase of the polymer-silicate interactions that slow the relaxation times of the PBT chains. Moreover, it was also evident that for the fillers having the higher affinity towards the PBT the nano-scale dispersion benefit from higher residence times, and therefore slower extrusion rates; on the contrary, for the fillers having poor interaction with the polymer, higher shear stress, and therefore higher extrusion rates, are needed to disrupt the clay tactoids in smaller particles. In the last part of the work, in order to verify if a relationship between flow properties and degree of exfoliation does actually exist, the rheological data were also processed using a simple semi-quantitative empirical method proposed in literature. The method failed for our systems, thus underlining the insufficiency of the rheological response alone in quantifying the exfoliation degree of an organoclay in the matrix.

Keywords: poly(butylene terephthalate); nanocomposites; melt rheology.

Introduction

Polymer-layered silicate nanocomposites are continuously gathering academic and industrial interest for their remarkable property improvements over the pristine polymer matrices; improvements that involve both functional (barrier properties and flame resistance) and structural properties (stiffness, dimensional stability, impact strength).

Many different processing routes are currently available to produce polymer-clay nanocomposites [1-7]. Among them, the most attractive is the melt compounding carried out in a shear device, that is relatively low-cost, adaptable to existing polymer processing plants and is environmentally sound (not requiring any solvent) [4-6].

The intercalation of polymer chains into the silicate galleries results from the concurrent effects of the chemical affinity between the polymer and the organo-modified silicate, and the shear stress transferred during the process. Both the chemical affinity and the processing conditions play a crucial role in the exfoliation and dispersion on a nanoscale level of the silicate layers into the polymer matrix [2, 5].

Melt compounding technique has been successfully used to process into nanocomposites many different kind of engineering plastics, like polyamides [6-8], polystyrene [9], polyolefines [10-11], poly(vinyl chloride) [4], poly(ethylene terephthalate) [12], but only few data have been reported, to date, on the direct melt intercalation of poly(butylene terephthalate) (PBT) nanocomposites [13-15]. PBT is a widely used engineering thermoplastic polymer characterized by a high rate of crystallization, good solvent resistance, thermal stability, and excellent processability and mechanical properties. The production of PBT-clay hybrids can potentially provide improved key properties like impact strength and heat distortion temperature, therefore increasing the industrial interest and widening the field of applicability of this polyester.

The main hindrance to the melt compounding of PBT hybrids is reportedly the likelihood of matrix degradation occurrence [2]. One cause of that phenomenon was identified in the decomposition reactions of alkyl ammonium cations in the organo-modified montmorillonites that can take place at processing temperatures above 200°C. Hence, a fine balance between processing temperatures, shear level, processing residence time and chemical affinity between clay and polymer is required in the melt blending of PBT in order to minimize those degradation phenomena and to get a good dispersion of the clay tactoids in the polymer matrix.

In our previous works [15-17] we obtained the melt intercalation of PBT into various kind of commercial modified montmorillonites differing by the organo-modifier employed, and we investigated the nano-scale morphology and the mechanical response of the obtained hybrids: our results showed clearly the strict dependence of the exfoliation efficiency and clay dispersion homogeneity upon the chemistry of the process, highlighting much higher exfoliation levels in the hybrids containing the clays whose organic modifiers may favorably interact with PBT matrix.

In this paper the relationships between composition, nanostructure and flow properties in melt compounded PBT-based nanocomposites have been further deepened: the melt rheology, already proven to be closely related to the material innermost morphology [2, 18-23], was again used as main investigation tool, together with supporting TEM analyses.

Different processing conditions and hybrid compositions have been considered in the preparation of the samples. In particular, the production of nanocomposites was carried out using a twin-screw extruder at two different extrusion rates. Four commercial organo-modified montmorillonites, differing mainly by the organic treatment used in the modification, were employed as nanometric fillers and blended with the PBT at two weight percentages each (6 and 9wt%). The nanocomposite samples were analyzed in terms of morphology and flow behavior. The rheological measurements were performed in the dynamic regime; the effect of temperature on the flow behavior of the hybrids with respect to the pristine PBT matrix was also investigated.

In the last part of the work, the obtained rheological data were also processed using a simple semi-quantitative empirical method proposed by R. Wagener et al. [24], in order to verify if a relationship between flow properties and degree of exfoliation does actually exist (as suggested in [24]) regardless of the different process and chemistry parameters (extrusion rates and/or organo-clay modifier type) employed in the production of the different samples.

Results and discussion

All PBT-based nanocomposite systems, prepared by melt compounding with four commercial organoclays at different clay loadings and extrusion rates, were submitted to morphological and rheological analyses in order to investigate the relationships between hybrid composition, exfoliation/dispersion level of the clay in the PBT matrix and viscoelastic response of the molten materials.

In Figure 1 the complex viscosity curves at 230°C for the PBT-100 and the samples extruded at 100 rpm and containing 6wt% of the four different fillers (Cloisite 25A, Cloisite 30B, Dellite 43B and Nanofil 919) are reported. As can be easily noted, the pseudo-Newtonian behavior of the neat PBT matrix changes into a very strong shear thinning trend in the hybrids, with almost divergent complex viscosity values at low frequency for all the four compositions examined. On the contrary, at high frequency all curves are almost superimposed, suggesting that the silicate layers are oriented in the flow direction in a high shear environment [2, 18] leaving essentially unaffected, the flow response of PBT. These results are consistent with a pseudo-solid-like behavior (at low ω) of the nanocomposite samples that can be related to meso-scale domain structures with long-range correlations defined by the highly anisotropic layered silicate [2]. The effect is much more marked in the hybrids containing the Nanofil 919 and the Dellite 43B fillers, whose curves are almost superimposed. These nanofillers, that include aromatic-based organo-modifiers, were already reported [16] as having higher affinity towards the polymer matrix with respect to the aliphatic-based Cloisites.

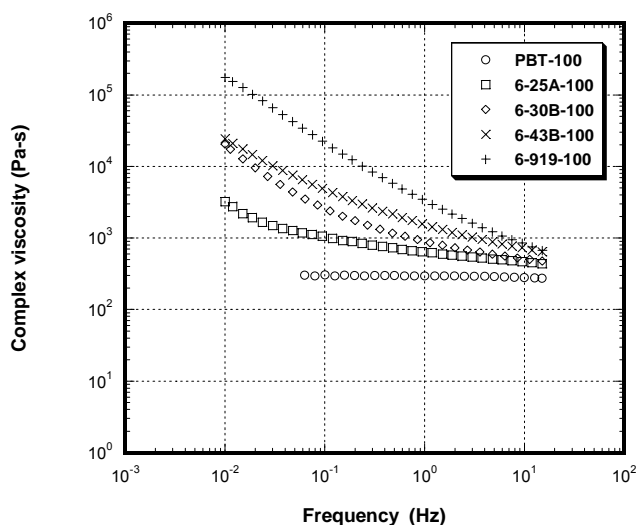


Fig. 1. Complex viscosity curves for neat PBT-100 matrix and for 6-25A-100, 6-30B-100, 6-43B-100 and 6-919-100 nanocomposites ($T=230^{\circ}\text{C}$).

To gain a better understanding of the factors affecting the exfoliation mechanisms of these two classes of nanofillers, the rheological investigation was deepened on the nanocomposites based on the Dellite 43B (aromatic modified) and the Cloisite 25A (aliphatic-modified): these two fillers have the same interstratic gap and mean grain size, thus differing only by the organo-modified type, as reported in Table 2.

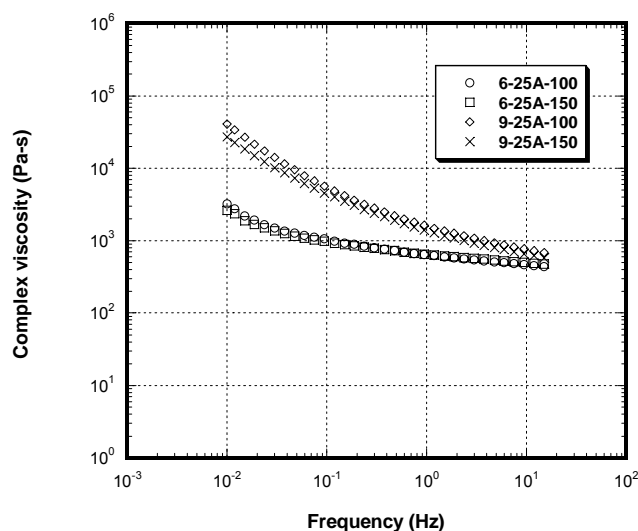


Fig. 2. Effect of clay loading and extrusion rate on the complex viscosity curves of Cloisite 25A-based nanocomposites ($T=230^{\circ}\text{C}$).

Figure 2 shows a comparison between the complex viscosity curves for samples 6-25A-100 and 6-25A-150 (a) and for samples 9-25A-100 and 9-25A-150, i.e. for samples having the same composition but processed using different extrusion rates (100 and 150 rpm). It is evident from the graphs that the change in the extrusion rate did not affect the flow behavior of these hybrids in a significant way; in fact, the flow curves related to samples extruded at 100 and 150rpm are actually almost superimposed. At a closer analysis, the complex viscosity curves of samples extruded at 150 rpm are slightly shifted towards lower η^* values than the ones related to samples processed at lower shear rate. These results point out that, for the PBT hybrids containing the 25A filler, an increase in the shear stress do not help the exfoliation process.

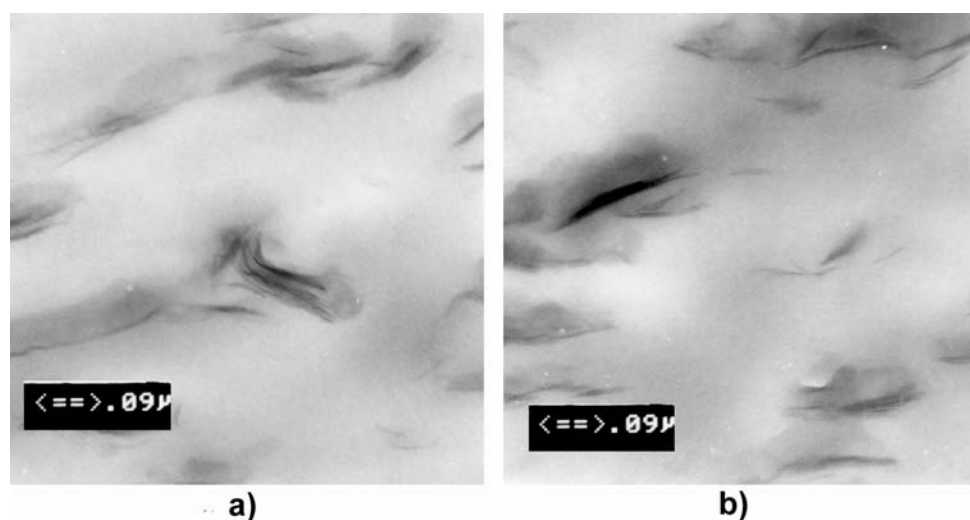


Fig. 3. TEM micrographs of 6-25A-100 (a) and 6-25A-150 (b).

Correspondingly to the rheological results, the comparison between TEM micrographs related to 6-25A-100 and 6-25A-150 (Figure 3a and 3b, respectively) and to 9-25A-100 and 9-25A-150 (Figure 4a and 4b, respectively) shows no significant structural differences between hybrids having same 25A contents but processed at different extrusion rates: the

same mixed intercalated/exfoliated structure can be noticed in both cases, with only a slight layer preferential orientation for samples processed at 150rpm. However, such orientation was disrupted during the annealing before the rheological tests and cannot cause the lowering in the complex viscosity values.

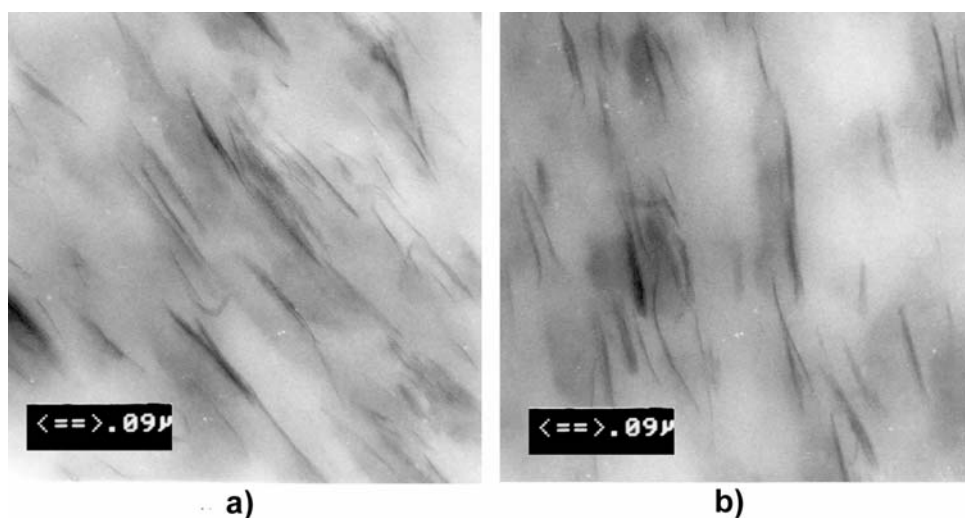


Fig. 4. TEM micrographs of 9-25A-100 (a) and 9-25A-150 (b).

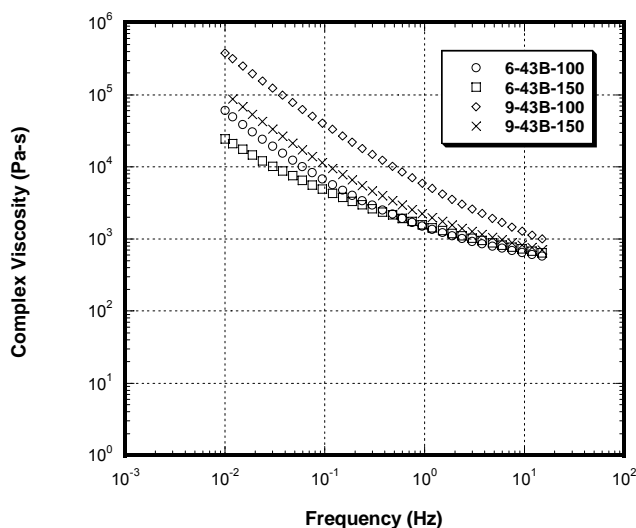


Fig. 5. Effect of clay loading and extrusion rate on the complex viscosity curves of Dellite 43B-based nanocomposites ($T=230^{\circ}\text{C}$).

Similar behavior was also observed for nanocomposites based on Dellite 43B organoclay, even if in this case the unfavorable effect of the shear rate on the nanoscale dispersion of the silicate is more evident. Figure 5 shows the dynamic response for samples containing 6wt% and 9wt% of Dellite 43B, extruded at 100 rpm and 150 rpm. The graph highlights that the samples extruded at lower extrusion rate have a more marked shear thinning behavior and higher complex viscosity values at all frequencies. Also this viscoelastic response can be associated to a higher degree of exfoliation in the nanocomposite samples extruded at lower rate. Again, this trend is backed by TEM analysis, depicted in Figures 6a-b and 7a-b, that highlights a far better dispersion and overall exfoliation in samples extruded at 100rpm.

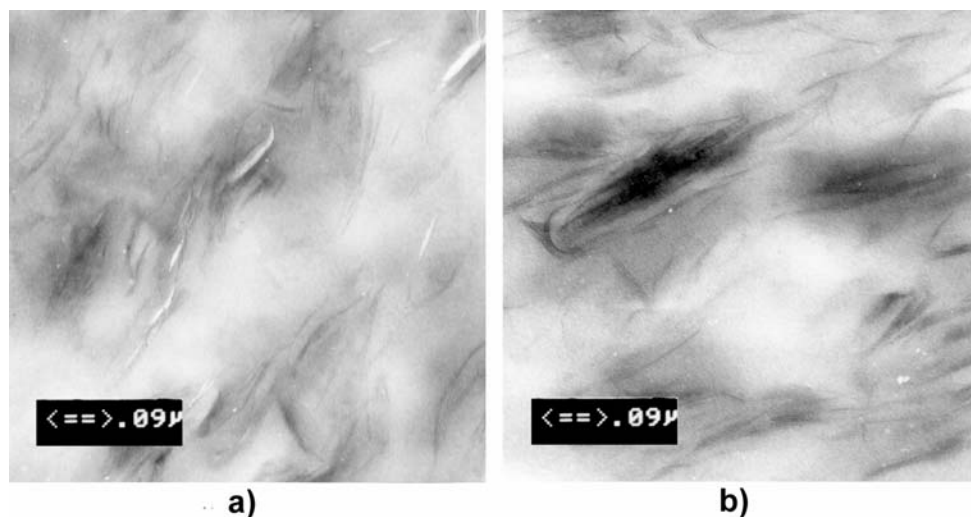


Fig. 6. TEM micrographs of 6-43B-100 (a) and 6-43B-150 (b)

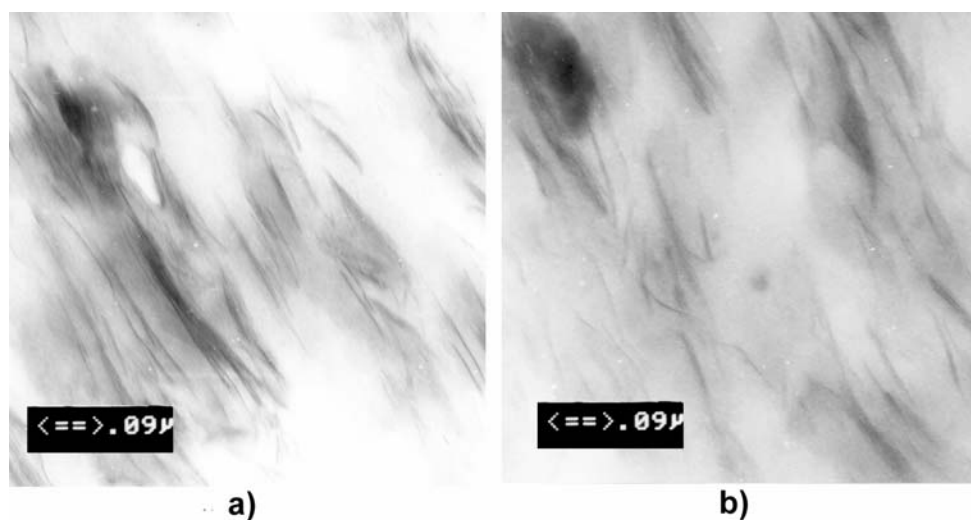


Fig. 7. TEM micrographs of 9-43B-100 (a) and 9-43B-150 (b)

To explain these trends in the rheological and morphological results, it is worthy to note that the intercalation/exfoliation degree of a silicate in a polymer matrix is the result from a balance of two main factors: the stress transferred from the molten polymer to the clay platelets, which disrupt the clay particle in platelet tactoids, and the polymer chain diffusion in the organoclay galleries, which leads to the “peeling” of individual layers from clay tactoids [25]. Supposedly, a lower level of shear and a higher residence time, resulting from the lower extrusion rate, lead to higher degrees of exfoliation in the final product with respect to the case of higher shear and lower residence time (condition associated with the higher extrusion rate). This can be due to the good affinity between the silicate and the PBT matrix, which particularly contributes to the intercalation of polymer chains via direct diffusion, and that benefit from the additional residence processing time. In support of these results, our previous work has shown the higher chemical affinity to the PBT of the Dellite 43B with respect to the Cloisite 25A) [16].

The effect of clay loading and extrusion rate on the viscoelastic response of the hybrids is even more detectable in the dynamic moduli curves, as shown in Figures 8a-b and 9a-b,

where the storage (G') and loss (G'') dynamic moduli of nanocomposite systems based on Cloisite 25A and Dellite 43B are reported, respectively.

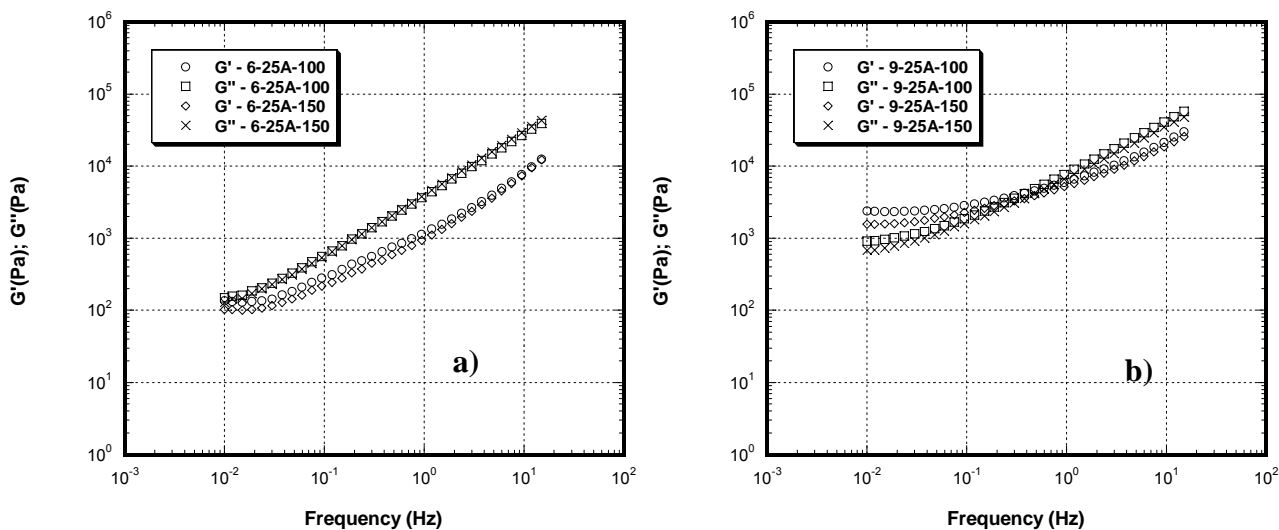


Fig. 8. Effect of the extrusion rate on the storage (G') and loss (G'') dynamic moduli for Cloisite 25A-based nanocomposite systems, at 6wt% (a) and 9wt% (b) of clay ($T=230^{\circ}\text{C}$).

Figures 8a-b show that for the Cloisite 25A-based hybrids both moduli increase at all oscillation frequency with the clay loading, but appear little sensitive to the extrusion rate, particularly at the lower silicate percentage. The dynamic spectra are dominated by the viscous response in all the frequency range examined in the case of the hybrids at 6wt% of clay. For the hybrids at 9 wt% of clay, instead, the predominantly elastic response at low frequency changes into a viscous one at $\omega > 0.4\text{Hz}$; moreover, at low ω both G' and G'' exhibit weak frequency dependence. These behaviors, confirming the gradual change of the behavior from pseudo-liquid-like to pseudo-solid-like after incorporating the clay in the PBT matrix, can be ascribed to the restricted segmental mobility of the polymer chains, more significant at higher clay loadings, at the PBT/clay interface neighborhood of the nanocomposites.

Similar trends in terms of frequency dependence can be observed in Figures 9a-b for the Dellite 43B-based hybrids at 6wt% and 9wt%. However, for these systems the pseudo-solid-like behavior is predominant up to $\omega = 0.7\text{Hz}$ for the 6wt% loaded samples and is predominant in the whole frequency range for the 9wt% samples.

Accordingly to complex viscosity data, these results confirm that increasing both the clay amount and the polymer/clay affinity, more highly constrained structures with more prevented relaxation motions of the polymer chains also arise.

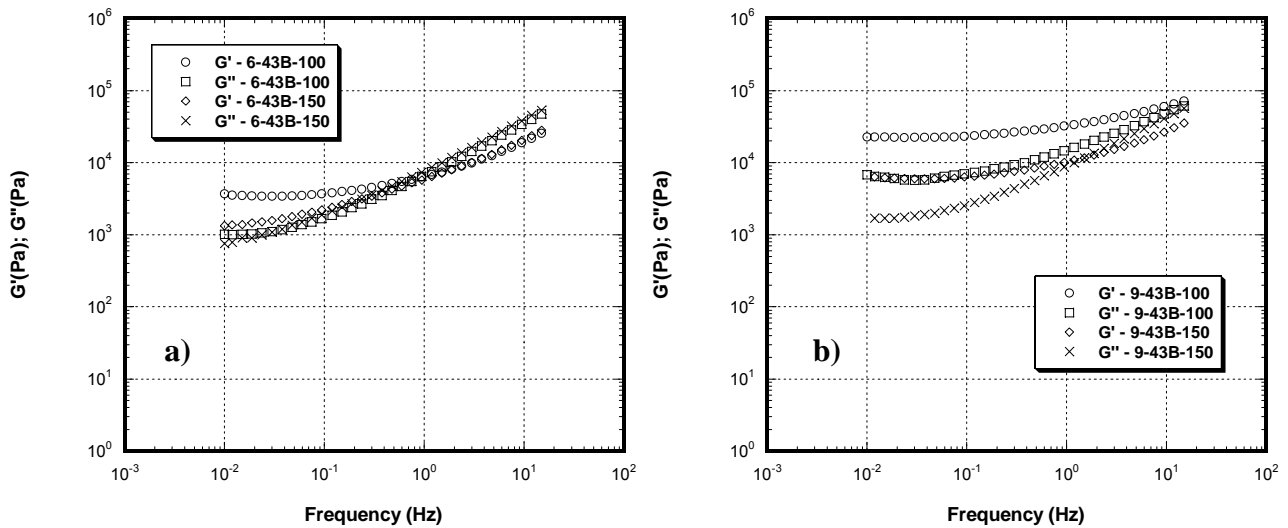


Fig. 9. Effect of the extrusion rate on the storage (G') and loss (G'') dynamic moduli for Dellite 43B-based nanocomposite systems, at 6wt% (a) and 9wt% (b) of clay ($T=230^{\circ}\text{C}$).

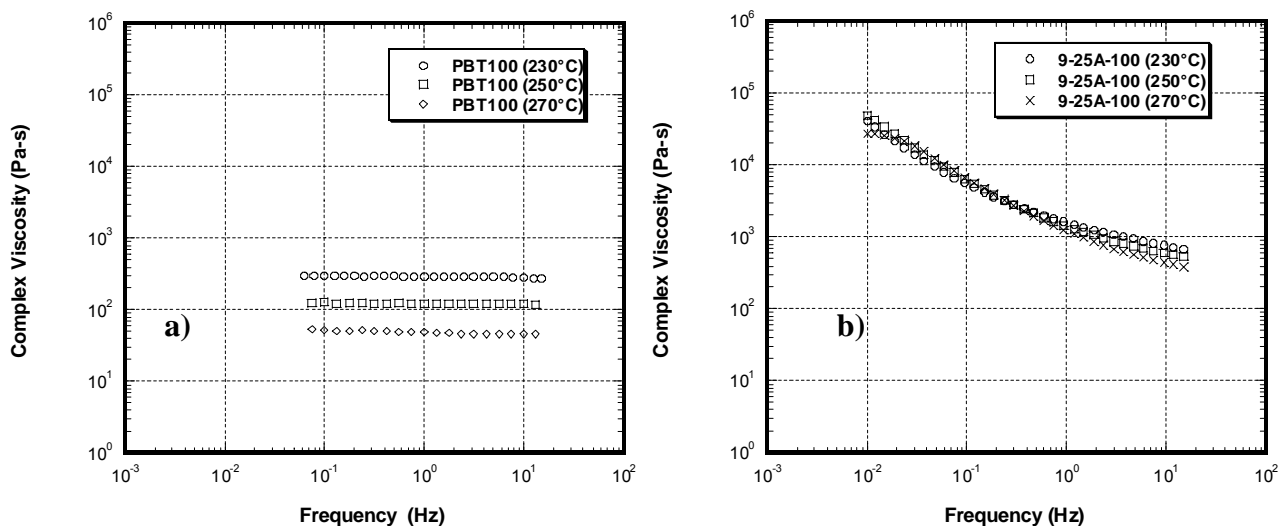


Fig. 10. Effect of the temperature on the complex viscosity curves of neat PBT-100 (a) and 9-25A-100 nanocomposite (b).

To further explore the effect of the nanoscale dispersion of percolated tactoids on the viscoelastic properties of nanocomposites, dynamic measurements at different test temperatures were conducted. Figure 10a-b respectively shows the complex viscosity curves for pure PBT-100 and the hybrid 9-25A-100 at three different test temperatures, namely 230, 250 and 270°C , while Figure 11a-b report the dynamic moduli curves for the hybrid 9-25A-100 at $T=230, 250$ and 270°C .

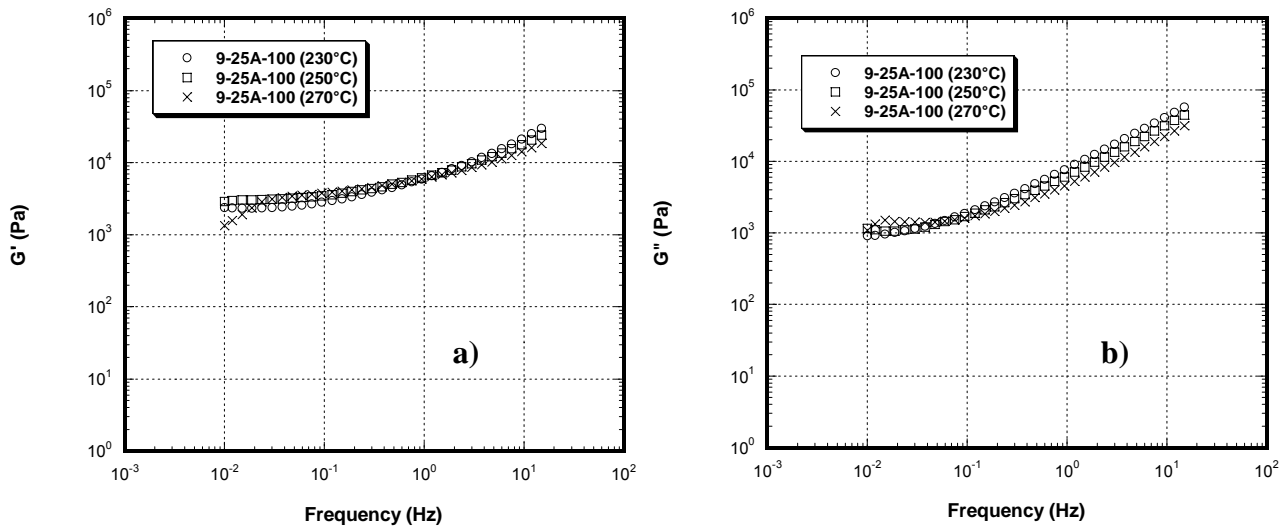


Fig. 11. Effect of the temperature on the dynamic moduli of 9-25A-100 nanocomposites: storage dynamic modulus G' (a) and loss dynamic modulus G'' (b).

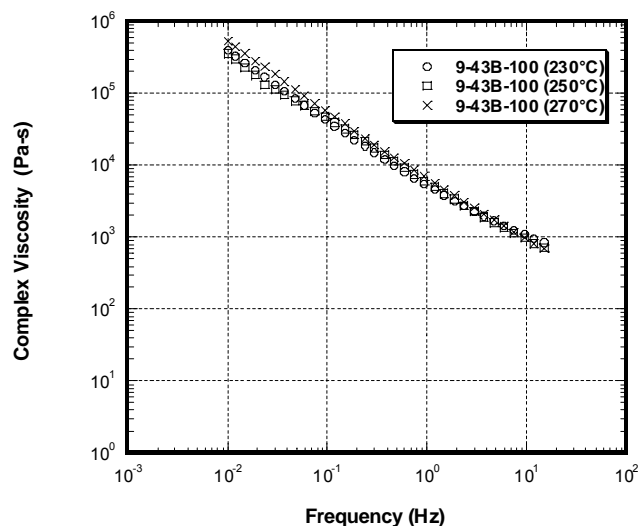


Fig. 12. Effect of the temperature on the complex viscosity curves of 9-43B-100 nanocomposites.

It can be easily noted that while the pure PBT-100 matrix has an Arrhenius-like temperature dependence, this is not the case for the hybrid, in which the complex viscosity is only slightly affected by the higher temperature. However, at the highest temperature investigated, the 6-25A-100 initially exhibits some shear-thickening behavior: such result may be related to a build-up of structure at low frequency, due to the further diffusion of PBT between the stacked clay layers promoted at high temperature; with increasing frequency this structure breaks down giving a shear thinning complex viscosity curve. A comparable trend can be observed in the temperature dependence of the η^* curves for the 9-43B-100 sample (Figures 12 and 13a-b), even if in this case their behavior is always shear-thinning.

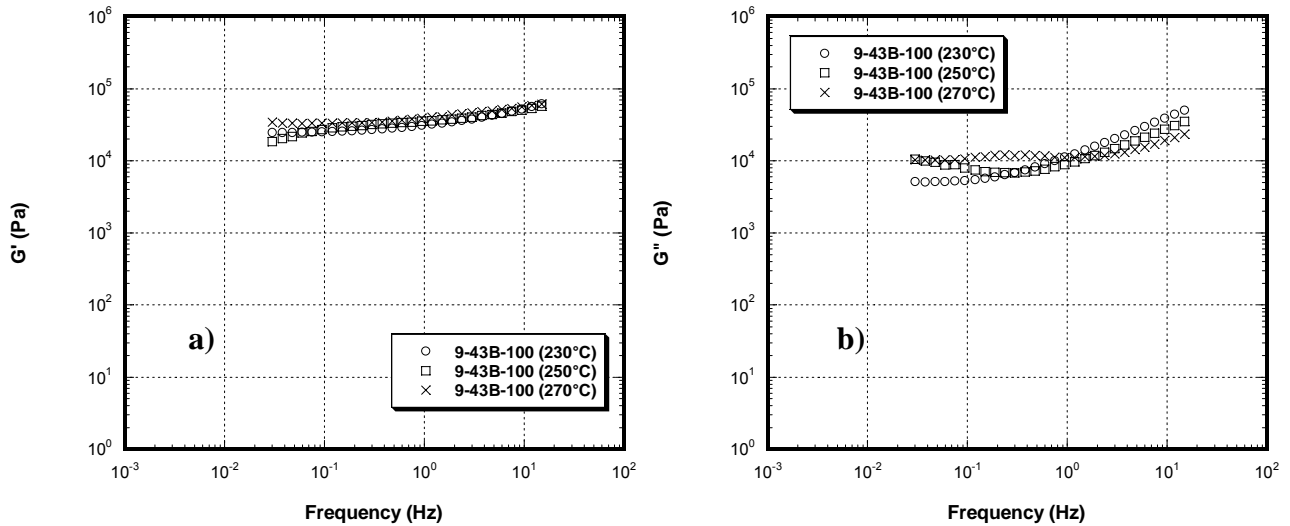


Fig. 13. Effect of the temperature on the dynamic moduli of 9-43B-100 nanocomposites: storage dynamic modulus G' (a) and loss dynamic modulus G'' (b).

The temperature independence exhibited by dynamic viscoelastic properties for the hybrids, as opposed to the Arrhenius-like temperature dependence of the neat matrix, further suggests that the linear viscoelastic properties in the nanocomposite samples are mainly dictated by the presence of a percolated network of nano-dispersed clay-platelet. Apparently, the relaxation of the interactions between the dispersed platelets does not occur in the examined temperature range. Further investigations are ongoing to clarify this rather interesting matter.

In order to systematically catalogue the rheological results and to spot a common trend among the different fillers, a semi-quantitative method, proposed by Wagener et al. [24] to evaluate the exfoliation/delamination degree of the clay in the polymer matrix from viscosity data, was applied to our experimental data.

According to this method, the shear thinning behavior of the complex viscosity curves can be used to quantify the nanodispersion level of the samples by fitting the η^* curves (in the low frequency region) to the power law expression:

$$\eta^* = A \cdot \omega^n \quad (1)$$

where η^* =complex viscosity, A =sample specific pre-exponential factor, ω =oscillation frequency and n =shear thinning exponent.

The shear thinning exponent allows a semi-quantitative discrimination between the different nano- and mesoscale composite structures formed by the clay platelets in the polymer matrix: when the η^* curve is practically horizontal (as for the neat PBT-100 matrix) $n > 0$ and continuously decreases with increasing the dispersion and exfoliation level of the clay sheets in the polymer.

Wagener et al. used this method to compare nanocomposite samples having the same composition (in terms of clay type and percentage) but prepared using different processing routes. They also suggested using it to directly compare systems prepared under varied conditions (e.g. nanoclay content, intercalant chemistry and extrusion rate), so we applied it to our rheological results in the dynamic regime. In Tab. 1 the shear thinning exponent values calculated for all our nanocomposite systems at different compositions extruded at 100 rpm are reported.

Tab. 1. Shear thinning exponent n , calculated according to eq.1, as proposed by Wagener et al. in [24].

Clay weight percentage (%)	Shear Thinning Exponent (n)			
	<i>Cloisite 25A</i>	<i>Cloisite 30B</i>	<i>Dellite 43B</i>	<i>Nanofil 919</i>
6	-0.432	-0.926	-0.701	-0.919
9	-0.823	-0.927	-0.964	-0.977
0	-0.008			

As expected, the shear thinning exponent values decrease coherently with the increase in the clay amount and the exfoliation level (already qualitatively inferred by TEM analysis). However, comparing these results with the complex viscosity curves of Figure 12 it is evident that 6-919-100 and 6-30B-100 samples, having similar n value and then similar shaped flow behavior, differ in the η^* values (taken at lowest frequency) by almost one order of magnitude. Such observation indicates that the semi-quantitative relationship between the rheological response and the nanostructure of PBT nanocomposites fails for these two systems, prepared using the same nanoclay content and extrusion rate but different intercalant chemistry. This result underlines the insufficiency of this rheological response alone in quantifying the exfoliation degree of an organoclay in the matrix.

Conclusions

In this study the melt flow behavior of poly(butylene terephthalate)–clay nanocomposites produced by melt compounding was investigated. Four commercial organo-modified montmorillonites, differing mainly by the organic treatment used in the modification, were employed as nanometric fillers and blended with the PBT at two weight percentages each (6 and 9wt%). The process was carried out using a twin-screw extruder at two different extrusion rates in order to evaluate the effects of shear rate during the process on microstructure and flow properties.

All samples were tested in order to analyze the relationships between composition (in terms of organoclay type and amount), morphology, processing conditions (extrusion rate) and rheological response. The nano-scale dispersion of the silicate into the polymer matrix was verified using TEM analysis. The more exfoliated clay dispersions were obtained with the Nanofil 919 and Dellite 43B organoclays, whose organic modifiers have a phenyl group that may determine favorable specific interactions with the aromatic rings of PBT chains.

The study showed evidence that, correspondingly to the more exfoliated morphologies, the viscoelastic response is characterized by markedly shear thinning complex viscosity curves, with a pseudo-solid-like flow behavior at long times, due to the occurrence of strong polymer-silicate interactions that slow the relaxation times of the polymer chains. The complex rheological behavior of these hybrids were further confirmed by the measurements performed at different temperatures: the tests illustrated that the complex viscosity is not strongly dependent on temperature, resulting in detectable changes in the flow curves that are probably related to temperature-induced meso-structural re-organizations.

The critical role of both polymer-organoclay affinity and processing conditions in determining an adequate exfoliation level during the melt compounding was also evidenced. Dynamic frequency sweep tests have shown that the increase in the screw speed rate - and then in the amount of shear stress involved in the process - does not improve the efficiency of the exfoliation process. Actually, in some cases, where a good

chemical affinity between the silicate and the matrix exists, a detrimental effect can be obtained, due to the reduced time given to the polymer for diffuse between the clay layers; this is the case of the Dellite 43B-based nanocomposites.

Finally, a semi-quantitative analytical method, proposed in literature to quantify the exfoliation level of polymer-silicate nanocomposites, was tested using our rheological data. Comparing the shear thinning indexes calculated for samples produced with the same clay loading and processing parameters but differing for the organo-clay chemistry, it was shown that viscoelastic measurements, although valuable tools to qualitatively probe the structure of nanocomposite materials, are insufficient to quantify the exfoliation degree of an organo-clay in the matrix.

Experimental part

Materials

The polymeric matrix used in this study was a poly(butylene terephthalate) (PBT TQ 904/N, Mn=28000) supplied by Montefibre (Italy). The commercial organoclays selected were Cloisite 25A, Cloisite 30B (produced by Southern Clay Products, Inc.), Dellite 43B (Laviosa Chimica) and Nanofil 919 (Süd Chemie). All those silicates are montmorillonite-based and were supplied as powders of particles nominally < 8µm in size, except for Nanofil 919 organoclay, whose particles have an average size of 35µm. The basic organoclay characteristics are summarized in Table 2.

Tab. 2. Basic characteristics of the commercial organoclays employed.

Trade name	Organo-modifier structure ⁽¹⁾	Organo-modifier concentration (meq/100g clay)	Basal spacing (Å)	Average medium size of particles (µm)
Cloisite 25A	$\begin{array}{c} \text{CH}_3 \\ \\ \text{H}_3\text{C}-\text{N}^+-\text{HT} \\ \\ \text{C}-\text{C}-\text{CH}_2\text{CH}_2\text{CH}_2\text{CH}_3 \\ \quad \\ \text{H}_2 \quad \text{CH}_2\text{CH}_3 \end{array}$	95	18.6	< 8
Cloisite 30B	$\begin{array}{c} \text{CH}_2\text{CH}_2\text{OH} \\ \\ \text{H}_3\text{C}-\text{N}^+-\text{T} \\ \\ \text{CH}_2\text{CH}_2\text{OH} \end{array}$	90	18.5	< 8
Nanofil 919	$\begin{array}{c} \text{CH}_3 \\ \\ \text{C} \\ \\ \text{H}_2 \end{array} \text{---} \text{C}_6\text{H}_5 \text{---} \text{N}^+ \text{---} \left[\text{CH}_2 \right]_{17} \text{---} \text{CH}_3$	90	19.5	35
Dellite 43B	$\begin{array}{c} \text{CH}_3 \\ \\ \text{C} \\ \\ \text{H}_2 \end{array} \text{---} \text{C}_6\text{H}_5 \text{---} \text{N}^+-\text{HT} \\ \\ \text{CH}_3$	95	18.6	< 8

⁽¹⁾HT is Hydrogenated Tallow (~65% C18; ~30% C16; ~5% C14) and T is Tallow (~65% C18; ~30% C16; ~5% C14)

Melt Processing

Mechanical polymer-silicate blends at two different weight percentages of each clay (6 and 9%) were prepared and dried in a vacuum oven at 90°C for 18 h to avoid moisture induced degradation reactions. The melt compounding of the blends was performed using a Haake

twin screw extruder having counter-rotating intermeshing conical screws (L=300mm). A temperature profile of 210-230-230-228°C from hopper to die was imposed in both the processing devices and a rectangular die (1mm x 40mm) was used. Nanocomposite tapes at two different organoclay contents were extruded at screw speed of 100 and 150 rpm, corresponding to an average residence time in the extruder of about 3.0 min and 1.6 min. Using the same processing conditions neat PBT tapes were also prepared for comparison. The samples nomenclature that will be adopted in the following for the hybrids is **X-CN-ER**, where **X** is the weight percentage of clay, **CN** is the clay commercial initials and **ER** is the extrusion rate expressed in screw rotation per minute; the neat PBT samples extruded at 100 and 150 rpm will be referred as **PBT-100** and **PBT-150**, respectively.

Before submitting the hybrids to the following study, the melt compounded samples were tested in order to verify the system composition in terms of clay loading and to assure the nanoscale dispersion of the clays into the polymer matrix.

In particular, to verify the correspondence between the nominal and the effective weight percentage of clay into the nanocomposite blends, all the extruded samples were submitted to thermo-gravimetric analysis under the conditions reported in the 'Methods' section. The obtained results are reported in Table 3. As it can be seen from the table, small differences (less than 10%) between the nominal and effective weight percentage of clay were found in all cases, proving that a good control on nanocomposite weight composition was achieved in our processing conditions. The effects of the differences between the nominal and the actual weight composition were not relevant for the discussion of the results, and will not be further mentioned in the following.

Tab. 3. Nominal and actual (measured) nanocomposite clay weight percentage.

Nominal weight percentage (%)	Actual measured weight percentage (%) $\pm \sigma$			
	<i>Cloisite 25A</i>	<i>Cloisite 30B</i>	<i>Dellite 43B</i>	<i>Nanofil 919</i>
6	5.7 \pm 0.5	5.9 \pm 0.3	5.8 \pm 0.2	6.2 \pm 0.2
9	9.2 \pm 0.4	9.1 \pm 0.4	8.9 \pm 0.4	9.1 \pm 0.3

Moreover, in order to investigate the sample morphology and nanoscale dispersion of clay platelets into the PBT matrix, transmission electron microscopy and X-ray diffraction measurements were performed. The results, already discussed in detail in our previous works [15-16] about the preparation of PBT-clay nanocomposites by melt compounding, show that all produced systems exhibit a mixed intercalated-exfoliated structure on a nanoscale level. The extent of exfoliation is found dependent upon the nanoclay type (with the higher affinity between organoclay and the matrix leading to better dispersion and exfoliation), weight composition and processing parameters. As an example, Figure 14 shows the x-ray diffractograms of 9-25A-100 and 9-43B-100 hybrids compared with those of the original 25A and 43B organoclays.

Comparing the XRD patterns, it can be observed that the characteristic basal reflection of the original organoclays is no more present in the hybrids and only a broad halo can be detected at decreasing 2θ , thus pointing out that the silicate interstratic gap is increased and the clay is dispersed on a nano-scale in the PBT. Similar results were obtained for all hybrids, irrespectively of clay concentration, indicating that a nano-scale dispersion of silicate layers have occurred in PBT matrix in the experimental conditions used.

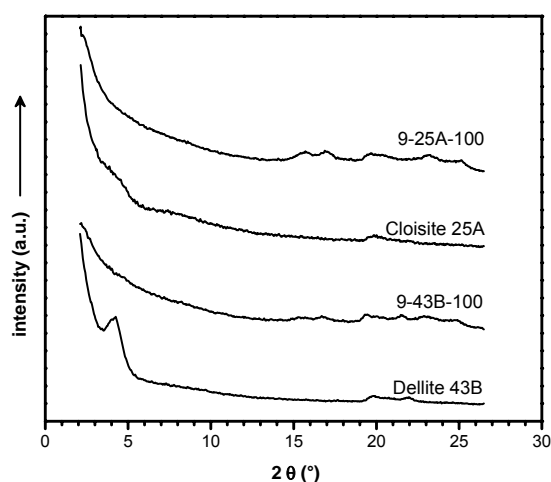


Fig. 14. XRD patterns of Cloisite 25A, Dellite 4B, 9-25A-100 and 9-43B-100 samples.

Methods

Thermo-gravimetric analyses (TGA) were carried out on all the clays, on neat PBT and on all the hybrids extruded with different clay contents and extrusion rates. TGA tests were performed using a TA TGA 2950 apparatus in the temperature range 25–900°C with a heating rate of 20°C/min under a nitrogen atmosphere.

X-ray diffraction spectra were recorded with a flat camera using a sample-to-film distance of 140 mm (Ni-filtered Cu-K α radiation). The Fujifilm MS 2025 imaging plate and a Fuji Bio-imaging Analyzer System, mod. BAS-1800, were used for digitizing the diffraction patterns. All spectra were taken on a ribbon section oriented normal to the extrusion direction.

Transmission electron microscopy (TEM) analysis was conducted using a Zeiss EM 900 operating at 80 kV. The images were captured on sections located normal to the extrusion direction prepared by cryogenically microtoming ultra-thin specimens (50 nm thick) using a Leica Ultracut UCT microtome operating at $T = -80^\circ\text{C}$.

The flow properties of the molten materials were measured in the dynamic regime with an ARES rheometer (Rheometrics, Inc.), using a parallel plates geometry (plate radius=12.5 mm, gap=0.1 mm), under a nitrogen gas purge. All measurements were performed with a force transducer having a range of 0.2–2000 g $_f$ -cm torque. The nanocomposite samples were dried at $T=90^\circ\text{C}$ in a vacuum oven for 18 h prior to testing, in order to minimize moisture-induced degradation phenomena at high temperature. Dynamic strain sweep tests were performed on all samples to select strain amplitude, 1%, that is within the linear viscoelastic response of the material. Then, dynamic frequency sweep tests were performed in the frequency range of $\omega=0.01$ –15 Hz, at $T=230^\circ\text{C}$, 250°C and 270°C . All tests were conducted after 5 min of annealing at the desired temperature, in order to erase the effects of eventual molecular orientations, induced during the extrusion process.

Acknowledgements

This work was supported by “Legge 449-97,” Project Title: Materiali compositi per applicazioni strutturali di rilevante interesse industriale.

References

- [1] Alexandre, M., Dubois, P.; *Mater. Sci. Eng.* **2000**; 28,1.
- [2] Pinnavaia, T.J., Beall, G.W. (eds); *Polymer-Layered Silicate Nanocomposites*, New York: John Wiley & Sons Ltd., **2001**.
- [3] LeBaron, P.C., Wang, Z., Pinnavaia, T.; *J. Appl. Clay Sci.* **1999**; 15, 11.
- [4] Lepoittevin, B., Pantoustier, N., Devalckenaere, M., Alexandre, M., Calberg, C., Jerome, R., Henrist, C., Rulmont, A., Dubois, P.; *Polymer* **2003**; 44, 2033.
- [5] Dennis, H.R., Hunter, D.L., Chang, D., Kim, S., White, J.L., Cho, J.W., Paul, D.R.; *Polymer* **2001**; 42, 9513.
- [6] Fornes, T.D., Yoon, P.J., Keskkula, H., Paul, D.R.; *Polymer* **2001**; 42, 9929.
- [7] Maa, J., Xub, J., Renb, J., Yua, Z., Maia, Y.; *Polymer* **2003**; 44, 4619.
- [8] Incarnato, L., Scarfato, P., Russo, G.M., Di Maio, L., Iannelli, P., Acierno, D.; *Polymer* **2003**; 44, 4625.
- [9] Vaia, R.A., Jandt, K.D., Kramer, E.J., Giannelis, E.P.; *Chem. Mater.* **1996**; 8(11), 2628.
- [10] Liu, X., Wu, Q.; *Polymer* **2001**; 42, 10013.
- [11] Nam, P.H., Maiti, P., Okamoto, M., Kotaka, T., Hasegawa, N., Usuki, A.; *Polymer* **2001**; 42, 9633.
- [12] Ke, Y.C., Long, C.F., Qi, Z.N.; *J. Appl. Polym. Sci.* **1999**; 71:1139-1146.
- [13] Wu, D., Zhou, C., Fan, X., Mao, D., Bian, Z.; *Polym. Degrad. Stab.* **2005**; 87, 511.
- [14] Wu, D., Zhou, C., Hong, Z., Mao, D., Bian, Z.; *Europ. Polym. J.* **2005**; 41, 2199.
- [15] Scatteia, L., Scarfato, P., Acierno, D.; *J. Plast. Rubber Compos.* **2004**; 33, 85.
- [16] Scarfato, P., Scatteia, L., Costa, G., Acierno, D.; *Macromol. Sym.* **2005**; 228, 125.
- [17] Acierno, D., Amendola, E., Costa, G., Scarfato, P., Nocerino, G.; *Polym. Eng. Sci.* **2004**; 44(6), 1012.
- [18] Khrishnamoorti, R., Yurekli, K.; *Curr. Op. Colloid Interface Sci.* **2001**; 6, 464.
- [19] Messersmith, P.B, Giannelis, E.P.; *J. Polym. Sci. Part A: Polym. Chem.* **1995**; 33, 1047.
- [20] Hyun, Y.H., Lim, S.T., Choi, H.J., Jhon, M. S.; *Macromolecules* **2001**; 34(23); 8084.
- [21] Kim, T.H., Jang, L.W., Lee, D.C., Choi H.J., Jhon, M.S.; *Macromol. Rapid Comm.* **2002**; 23(3), 191.
- [22] Lim, S.T., Lee, C.H., Choi H.J., Jhon, M.S; *J. Polym. Sci. Part B: Polym. Phys.* **2003**; 41(17), 2052.
- [23] Lim, S.T., Hyun, Y.H., Choi, H.J., Jhon, M.S.; *Chem. Mater.* **2002**; 14(4); 1839
- [24] Wagener, R., Reisinger, T.J.G.; *Polymer* **2003**; 44, 7513.
- [25] Cho, J.W., Paul, D.R.; *Polymer* **2001**; 42, 1083.